Development 133, 1347-1357 doi:10.1242/dev.02306

The developing lamprey ear closely resembles the zebrafish otic vesicle: *otx1* expression can account for all major patterning differences

Katherine L. Hammond and Tanya T. Whitfield*

The inner ear of adult agnathan vertebrates is relatively symmetric about the anteroposterior axis, with only two semicircular canals and a single sensory macula. This contrasts with the highly asymmetric gnathostome arrangement of three canals and several separate maculae. Symmetric ears can be obtained experimentally in gnathostomes in several ways, including by manipulation of zebrafish Hedgehog signalling, and it has been suggested that these phenotypes might represent an atavistic condition. We have found, however, that the symmetry of the adult lamprey inner ear is not reflected in its early development; the lamprey otic vesicle is highly asymmetric about the anteroposterior axis, both morphologically and molecularly, and bears a striking resemblance to the zebrafish otic vesicle. The single sensory macula originates as two foci of hair cells, and later shows regions of homology to the zebrafish utricular and saccular maculae. It is likely, therefore, that the last common ancestor of lampreys and gnathostomes already had well-defined otic anteroposterior asymmetries. Both lamprey and zebrafish otic vesicles express a target of Hedgehog signalling, *patched*, indicating that both are responsive to Hedgehog signalling. One significant distinction between agnathans and gnathostomes, however, is the acquisition of otic *Otx1* expression in the gnathostome lineage. We show that Otx1 knockdown in zebrafish, as in *Otx1*$^{-/-}$ mice, gives rise to lamprey-like inner ears. The role of Otx1 in the gnathostome ear is therefore highly conserved; otic *Otx1* expression is likely to account not only for the gain of a third semicircular canal and crista in gnathostomes, but also for the separation of the zones of the single macula into distinct regions.

KEY WORDS: Lamprey, Zebrafish, Agnathan, Gnathostome, Inner ear, Otic vesicle, Macula, *follistatin*, *ptc*, *otx*, Evolution, Placode, Hair cell, Planar polarity pattern

INTRODUCTION

The vertebrate inner ear is required not only for hearing, but also for the sensation of position and movement in three-dimensional space. To accomplish this, it has evolved in gnathostome (jawed) vertebrates into a complex structure that is highly asymmetric about all three body axes (anteroposterior, dorsoventral and mediolateral), enabling sensitivity to head movement in any direction (Fig. 1). All gnathostome inner ears have three orthogonally arranged semicircular canals, their associated cristae, and a number of other patches of sensory epithelium. Depending on the species, these usually include the utricular, saccular and lagenar maculae, together with any specialised auditory endorgans (amphibian papilla, basilar papilla, organ of Corti). We set out to address the mechanisms underlying the evolution of this complexity of pattern in the vertebrate lineage.

Gnathostome vertebrates and the few remaining extant agnathan (jawless) vertebrates (lampreys and hagfish) are thought to have evolved from a common agnathan ancestor. Inner ear morphology underwent a significant change at the agnathan/gnathostome transition. The inner ears of adult agnathan fish are, at least superficially, more symmetrical about the anteroposterior (AP) axis than those of gnathostomes (Fig. 1). Adult lamprey inner ears have only two semicircular canals, each with a tricuspid crista, and a single ventrally positioned macula communis that covers the floor of two joined, symmetrical, ciliated chambers (de Burlet and Versteegh, 1930; Lowenstein et al., 1968; Thornhill, 1972; Avallone et al., 2005). A similar pattern, with two semicircular canals, is found in the abundant agnathan fossil record, making it likely that this represents the ancestral condition (Mazan et al., 2000). Hagfish also have a single macula communis on the ventral floor of the inner ear, but differ in having a single toroidal semicircular canal, which nevertheless is associated with two cristae, and is probably a derived characteristic (Lowenstein and Thornhill, 1970) (for a review, see Lowenstein, 1971). Although the general appearance of the inner ear is symmetrical about the AP axis in adult agnathan fishes, the macula communis can be subdivided into at least three morphologically distinct regions, the anterior horizontal, vertical and posterior horizontal regions (Lowenstein et al., 1968; Lowenstein and Thornhill, 1970; Hagelin, 1974), and there have been several different interpretations of the homology of these regions to the various gnathostome maculae (de Burlet and Versteegh, 1930; Lowenstein et al., 1968; Thornhill, 1972; Hagelin, 1974). Several studies describe hair cell planar polarity patterns in the late larval and adult lamprey and hagfish macula communis as roughly symmetrical about the AP axis (Lowenstein et al., 1968; Lowenstein and Thornhill, 1970; Thornhill, 1972), and Hagelin (Hagelin, 1974) tentatively proposes that both the anterior and posterior ends of the lamprey macula correspond to the gnathostome utricular macula. Although these homologies are not completely resolved, the relative symmetry of the adult agnathan ear suggested to us that the asymmetric gnathostome ear might have evolved from a more primitive symmetric form.

Although the gnathostome otic vesicle shows distinct asymmetry from early stages, studies in amphibian, mouse and zebrafish embryos have suggested that the anterior and posterior ends of the otic vesicle are initially equipotential, and that the ear is capable of developing as a more symmetric structure following physical or

Centre for Developmental and Biomedical Genetics, Department of Biomedical Science, University of Sheffield, Sheffield S10 2TN, UK.

*Author for correspondence (e-mail: t.whitfield@sheffield.ac.uk)

Accepted 1 February 2006

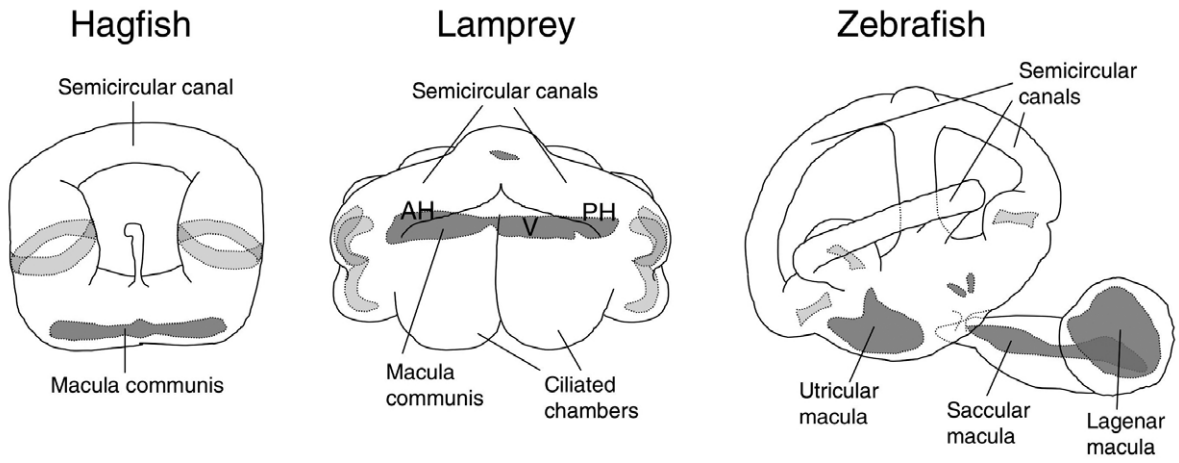

Fig. 1. Comparative sketch of adult hagfish, lamprey and zebrafish inner ears. Lateral views with anterior to the left; not to scale. Sensory maculae are shown in dark grey; cristae are shown in light grey. Note the single macula communis in the hagfish and lamprey ear, and the asymmetric arrangement of three separate sensory maculae in the zebrafish ear. AH, V and PH are the anterior horizontal, vertical and posterior horizontal regions, respectively, of the lamprey macula communis. (Adapted from diagrams in Gegenbaur, 1898; de Burlet and Versteegh, 1930; Lowenstein, 1971; Hagelin, 1974; Bang et al., 2001.)

genetic manipulation of the embryo (Harrison, 1936; Harrison, 1945; Waldman et al., 2001; Léger and Brand, 2002; Raft et al., 2004). We have shown that disruptions of Hedgehog (Hh) signalling in the zebrafish embryo give rise to an ear that is more symmetric about the AP axis. Specifically, a loss of Hh signalling in the embryo results in an enantiomorphic (mirror image) ear with double anterior character, whereas overactivity of the Hh pathway results in a double posterior ear (Hammond et al., 2003). In both cases, a single mirror-image, twinned macula can be produced, reminiscent of the single macula communis in the agnathan ear.

It has been suggested that mutations such as these, resulting in a loss of asymmetry in the gnathostome ear, may represent an atavistic reversion to a more primitive state (Léger and Brand, 2002). Such an interpretation rests upon the assumption that the relative symmetry of the adult agnathan ear is reflected in its development. A prediction of this idea is that the agnathan otic vesicle develops in a symmetric manner, lacking the asymmetric expression of marker genes seen in the zebrafish. It might also be expected that the agnathan otic vesicle is unresponsive to polarising signals known to be important in zebrafish, such as Hh signalling. To test these ideas, we have examined ear development in the lamprey, at both morphological and molecular levels. We have concentrated on the morphology and planar polarity patterns of the developing macula communis, and the expression of genes for which the zebrafish homologue is expressed in a polarised fashion in the otic vesicle. Contrary to our expectation, we find that the otic vesicle of the lamprey displays many similarities to that of zebrafish, including considerable morphological and molecular asymmetry about the AP axis; thus the apparent symmetry of the adult agnathan ear belies an asymmetric developmental programme. We also show that the lamprey otic vesicle expresses a homologue of *patched*, suggesting that it is responsive to Hh signalling, and indicating that a new role for Hh signalling in the ear probably did not account for the evolution of additional complexity in inner ear morphology at the agnathan/gnathostome transition.

In addition to extrinsic patterning information, transcription factors expressed within the otic epithelium have cell autonomous functions in otic patterning. A role for Otx1 has already been implicated in the appearance of the third, horizontal semicircular canal and crista in the gnathostome ear (Tomsa and Langeland, 1999; Mazan et al., 2000). An *otx* gene is not expressed in the lamprey ear (Ueki et al., 1998; Tomsa and Langeland, 1999). In gnathostomes, however, *Otx1* is expressed in a region that gives rise to the horizontal semicircular canal and crista, and is critical for their formation; in mice homozygous for a targeted disruption of *Otx1*, the horizontal canal and crista are absent, and the utricle fails to separate properly from the saccule (Acampora et al., 1996; Morsli et al., 1999; Fritzsch et al., 2001). We show that a knockdown of Otx1 function in the zebrafish embryo has similar effects on the ear to those seen in the mouse, confirming that the acquisition of otic *otx1* expression at the agnathan/gnathostome transition was likely to have been responsible, not only for the appearance of the horizontal canal and crista, but also for the separation of distinct areas of sensory tissue from an ancestral (but already polarised) macula communis.

MATERIALS AND METHODS

Collection and observation of embryos

Lamprey

Lampetra planeri eggs were collected from streams in the New Forest, UK (April 2003); *L. fluviatilis* eggs were collected from the rivers Nidd and Skell (North Yorkshire, UK, April 2004, April 2005). Embryos were cultured at 18°C in filtered river water containing 0.0001% methylene blue and staged according to Tahara (Tahara, 1988). Live observation was carried out as for zebrafish (Westerfield, 1995). Dechorionated embryos were fixed overnight at 4°C in 4% paraformaldehyde in 1×PBS, washed several times in PBS, and either stored at 4°C in 1×PBS, 0.1% sodium azide for FITC-phalloidin staining and immunohistochemistry, or dehydrated through a methanol series and stored at –20°C in 100% methanol for in situ hybridisation. Fixed *Petromyzon marinus* embryos, collected at the Hammond Bay Biological Station, MI, USA, were kindly provided by Dr David McCauley, Caltech (McCauley and Bronner-Fraser, 2002).

Zebrafish

WIK embryos were cultured as previously described (Westerfield, 1995). Observation of live embryos and fixation were carried out as for lamprey embryos.

Photography

Examination and photography of live and fixed samples were carried out using an Olympus BX51 compound microscope, Olympus Camedia (C-3030Z00M) camera and AnalySIS software (Olympus). Images were assembled with Adobe Photoshop.

FITC-phalloidin staining and immunohistochemistry

Fixed embryos were stained whole with FITC-phalloidin (Sigma) as described by Haddon and Lewis (Haddon and Lewis, 1996), except that lamprey embryos were permeabilised in 2% Triton in 1×PBS for five days at 4°C. Double staining using FITC-phalloidin and anti-acetylated tubulin antibody (Sigma) was performed essentially as described by Haddon and Lewis (Haddon and Lewis, 1996), but lamprey ears were dissected out and permeabilised for 30-60 minutes in 1% Triton at room temperature before staining. Zebrafish embryos were permeabilised in 1% [24-30 hours post-fertilisation (hpf)] or 2% (72 hpf +) Triton at room temperature for three hours and stained whole. Samples were mounted in Vectashield (Vector Laboratories) and imaged on a Leica SP confocal microscope.

Isolation and sequencing of lamprey cDNA

A 747 bp *ptc* fragment was amplified from a 6- to 10-day-old *P. marinus* embryo oligo (dT)-primed lambda ZapII cDNA library (a gift from J. Langeland, Kalamazoo College) by degenerate PCR, using the primers 5′-tcacccctctggactgcttytgggargg-3′ (forward) and 5′-gcacctgggtggtggcngcrt-traa-3′ (reverse), followed by a semi-nested PCR reaction with an internal reverse primer, 5′-cggacaagcacaccagcarnacnccngc-3′, and the forward primer from the first reaction. A 301 bp *follistatin* fragment was amplified from *L. fluviatilis* oligo (dT)-primed stage 22/23 cDNA by degenerate PCR (primers: forward, 5′-acacagtgcaggctggaaaytgytggyt-3′; reverse, 5′-tgttg-gagcagtcaggagcrcanacrca-3′). RNA was extracted from stage 22/23 *L. fluviatilis* embryos using Trizol (Sigma). cDNA was transcribed using a Superscript III first strand synthesis kit (Invitrogen) and PCR was carried out using Diamond Taq polymerase for GC-rich DNA (Bioline). PCR fragments were cloned into pGEM T-Easy using a T-Easy cloning kit (Promega) and used to screen the *P. marinus* cDNA library. [^{32}P]dCTP-labelled probes were made from these PCR fragments and the library screened as described previously (Nehls et al., 1994). Phagemid was excised from isolated plaques using ExAssist helper phage (Invitrogen). A single 1502 bp partial *ptc* clone and two *follistatin* clones (1227 bp and 1886 bp, both containing the full ORF) were obtained. A 538 bp *fgf8/fgf17* fragment was also amplified by PCR from *L. fluviatilis* cDNA (primers: forward, 5′-caaactgaccgtggaaacgg-3′; reverse, 5′-ccctccctcctgcggcgtc-3′). Sequencing was performed by the Genetics Core Facility, University of Sheffield, using an ABI 3730 capillary sequencer and analysed using the The Biology WorkBench (http://workbench.sdsc.edu).

Sequences for *P. marinus patched*, *P. marinus follistatin* (*long*), *P. marinus follistatin* (*short*) and *L. fluviatilis fgf8/fgf17* have been deposited in GenBank with Accession numbers DQ370170, DQ370171, DQ370172 and DQ370173, respectively.

In situ hybridisation

Digoxigenin-labelled probes were synthesised using a DIG labelling kit (Roche). Antisense and sense riboprobes were made from linearised full-length *L. fluviatilis tbx1* cDNA (Sauka-Spengler et al., 2002), our *P. marinus follistatin* cDNA and the partial *P. marinus ptc* cDNA, together with an antisense probe to our *L. fluviatilis fgf8/fgf17* fragment. In situ hybridisation to lamprey embryos was carried out essentially as described by Tomsa and Langeland (Tomsa and Langeland, 1999). For photography, stained lamprey embryos were dehydrated through an ethanol series and cleared and mounted in Murray's clear (2:1 benzyl benzoate:benzyl alcohol). In situ hybridisation to zebrafish embryos was carried out as described previously (Hammond et al., 2003). Zebrafish embryos were cleared and mounted in glycerol and photographed as above. All sense hybridisations were negative.

Morpholino injections to zebrafish embryos

An antisense morpholino (GeneTools, sequence 5′-taacatatagcctacctgaactcgg-3′) was targeted to the exon 3/intron 3-4 junction of the zebrafish *otx1* gene (GenBank Accession number NM 131250/ Ensembl reference ENSDARG00000043643, Zv5). Approximately 5 nl of 0.66 mM or 1.00 mM morpholino was injected into one- or two-cell embryos using a Narishige microinjection rig. To test for disruption of splicing, RT-PCR was performed (primers: exon 2 forward, 5′-atggacctactacacccgtc-3′; exon 4 reverse, 5′-gtgctgagcctggagaaatg-3′). RNA was extracted from pools of 25 24 hpf, 50 hpf, 74 hpf or 4 days post-fertilisation (dpf) embryos (either uninjected, or injected with 5 nl of 1 mM morpholino) using Trizol (Sigma), and cDNA was transcribed using a Superscript III first strand synthesis kit (Invitrogen). PCR was carried out using Taq polymerase (Promega). The 447 bp band represents correctly spliced *otx1* mRNA; the 471 bp and 408 bp bands represent aberrantly spliced forms, where splicing has occurred from cryptic donor sites 39 bases 5′ or 24 bases 3′ of the correct exon 3 donor site. This was confirmed by sequencing the PCR products using internal primers (exon 3 forward, 5′-agaggactacatttacgcgct-3′; exon 4 reverse, 5′-ctgtgttattggtggaggaag-3′). PCR was also carried out using gene-specific primers (forward, 5′-aagcaggagtacgatgagtctg-3′; reverse, 5′-ggtaaacgcttctggaatgac-3′) to amplify actin cDNA as a positive control.

Fluorescent labelling of the otic vesicle lumen

Embryos at 4 dpf were anaesthetised, immobilised in 1.0% low melting point agarose and fluorescein-conjugated morpholino injected into the lumen of the ear using a Narishige microinjection rig. Injected ears were imaged on a Leica SP confocal microscope within a few minutes of injection.

RESULTS

The embryonic lamprey ear is morphologically asymmetric about the AP axis

To examine the morphology of the developing lamprey inner ear, we observed live embryos of *Petromyzon marinus* (sea lamprey), *Lampetra fluviatilis* (river lamprey) and *Lampetra planeri* (brook lamprey) with DIC optics at stages 24 to 30, and stained fixed samples with FITC-phalloidin. FITC-phalloidin marks cortical actin in every cell, and highlights the actin-rich stereocilia of sensory hair cells, allowing general ear morphology and sensory maculae to be visualised. We find that the inner ears of all three species develop similarly, although there are slight differences in size and proportion between species at equivalent stages. Here, we concentrate on *L. fluviatilis* (Figs 2-4); data for *L. planeri* and *P. marinus* are provided as supplementary material, see Figs S1, S2.

At stage 24 (approximately 8 dpf), the lamprey inner ear consists of a simple epithelial vesicle; a small dorsal outpocketing that will form the endolymphatic duct is just visible (Fig. 2A,A′), and anteroventral cells are beginning to delaminate to form the statoacoustic (VIIIth) ganglion (Fig. 2A′,D). By stage 25 (10-11 dpf), hair cells develop in two discrete regions at the anterior and posterior ends of the vesicle, forming first at the posterior and then a short time later at the anterior (Fig. 2B,C,C′). These are the first AP asymmetries seen within the otic vesicle. By stage 26 (11-12 dpf), a well-defined group of hair cells is present at each end of the vesicle and the endolymphatic duct is obvious in the dorsal roof of the ear (Fig. 2D,D'). The statoacoustic ganglion can be visualised at stages 26-27 with anti-acetylated tubulin antibody (Fig. 2E,E′), and remains in a similar anteroventral position with respect to the vesicle until at least stage 29.

Although the lamprey otic vesicle forms by invagination of placodal ectoderm (Thornhill, 1972; Hagelin, 1974), in contrast to the cavitation seen in zebrafish (Haddon and Lewis, 1996), there are parallels between the two species at these early otic vesicle stages. In both species, neuroblasts migrate from ventral regions of the vesicle to form the statoacoustic ganglion anteroventral to the ear, and hair cells develop in two distinct groups at the anterior and posterior of the vesicle (Haddon and Lewis, 1996) (Fig. 2H,I). The endolymphatic duct, however, does not begin to form until later in the zebrafish, and is never as obvious as in the lamprey (L. Abbas, K.L.H., C. Mowbray and T.W., unpublished).

At stage 27 (13-15 dpf), hair cells start to develop medially between the two initial groups in the lamprey otic vesicle (Fig. 2F,F′). Subsequently, hair cell number continues to increase, forming a sensory patch that folds anteriorly onto the vertical

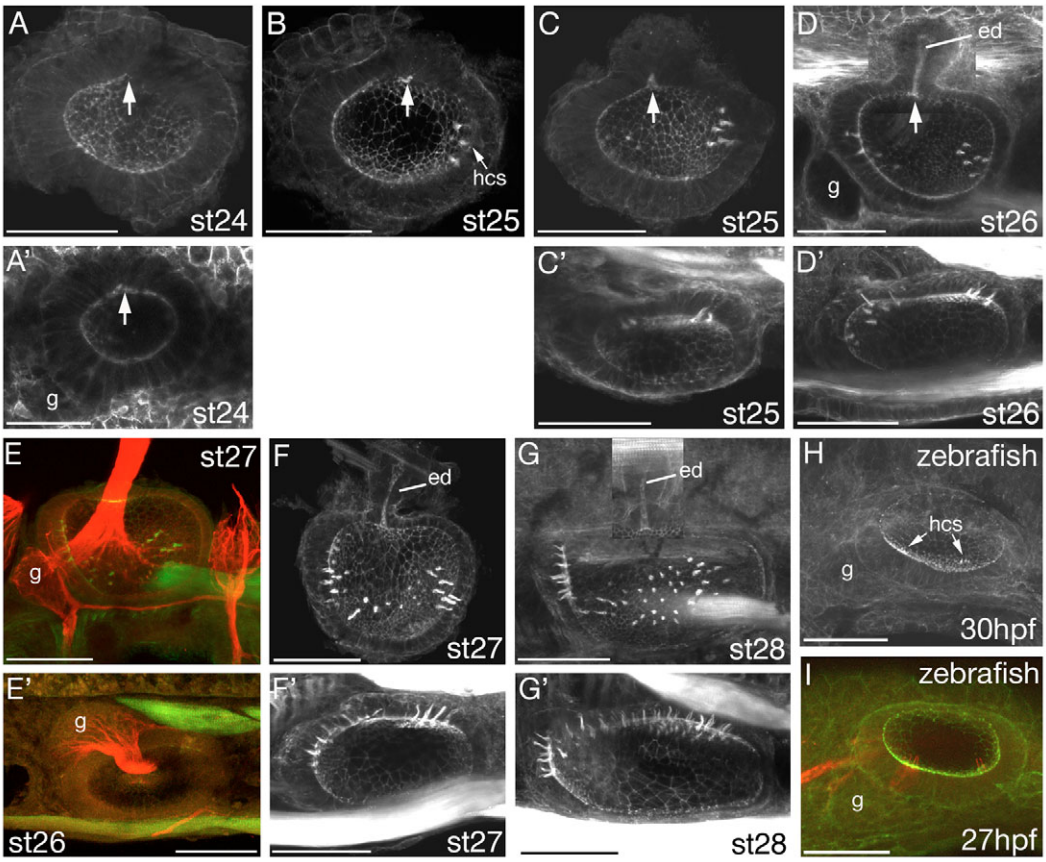

Fig. 2. Early development of the lamprey otic vesicle. (**A-I**) Projections of confocal *z*-stacks of embryos stained with FITC-phalloidin, revealing the actin-rich stereocilia of the sensory hair bundles and the general morphology of the developing lamprey inner ear. All images are of *L. fluviatilis*, except for A′ (*L. planeri*) and H,I (zebrafish). (A-I,A′) Lateral views, anterior to the left, dorsal to the top; (C′-G′) dorsal views, anterior to the left, medial to the top. (A-C,E,F) Partially dissected specimens; (D,G) composites of two images. Arrows indicate outpocketing of endolymphatic duct. g, statoacoustic (VIIIth) ganglion; ed, endolymphatic duct; hcs, sensory hair cells. (E,E′,I) Double stains with FITC-phalloidin (green) and anti-acetylated tubulin (red) to reveal neuronal cell bodies and axonal projections of the statoacoustic ganglion (E,E′) and sensory hair cell kinocilia (I). Stages are shown for each panel. Scale bars: 50 μm.

anterior wall and posteriorly onto the ventromedial wall, demonstrating significant AP asymmetry within the otic vesicle (Fig. 2G,G′, Fig. 3A-A′′). Although this patch appears to be a single sensory region (a 'macula communis') by stage 29 (18 dpf), hair cell density within it is variable: an anterior region of high cell density and a posterior region of high cell density are linked by a much more sparsely populated region (Fig. 3G,H). This is especially obvious at stage 28 (16-17 dpf), and is also reflected in the arrangement of otoconia that can be observed in live embryos (Fig. 3B-E). The otoconia sit over the macula, forming an otoconial mass, which at stage 28 – and to a lesser extent at stage 29 – is variably split at the region of lower hair cell density, creating two distinct otoconial masses overlying the anterior and the posterior portions of the macula (Fig. 3D,E). Taken together, these data suggest that although this sensory patch has been termed a macula communis, it consists of at least two distinct morphological regions, evident from early stages.

Our data differ from those of Hagelin, who suggests that there are three separate otoconial masses (Hagelin, 1974); however, his observations were made at later stages than ours, and it is conceivable that the otoconial masses later subdivide (Hagelin, 1974). Lowenstein et al., however, report only a single otoconial mass, even in the adult (Lowenstein et al., 1968). We believe that our observations of otoconia in the live embryo are likely to be more reliable than those made on fixed material, but unfortunately such live observations are limited to stages when the embryo is relatively optically clear.

At stage 29, there is no obvious sign of semicircular canal formation or crista development in the lamprey ear. However, at stage 30, we have observed what we interpret to be the beginnings of crista formation in two stage 30 *L. fluviatilis* ears (Fig. 4); epithelial projections also begin to form the semicircular canal system at this stage. We have not observed any hair cells that obviously correspond to the dorsal macula in the lamprey (Lowenstein et al., 1968; Thornhill, 1972; Hagelin, 1974).

Distinct regions of the lamprey macula communis correspond to the utricular and saccular maculae of zebrafish

Based on their initial appearance and position within the otic vesicle, the anterior and posterior regions of high cell density in the developing lamprey macula communis bear a distinct resemblance to the developing utricular and saccular maculae, respectively, of the zebrafish ear (Fig. 3F,I). To investigate these putative homologies further, we set out to map hair cell polarity patterns in the lamprey macula communis. Sensory patches within the ear have stereotypical patterns of hair cell planar polarity, specific to both a given species and a particular type of patch. A confocal optical section at the level of the apical membrane of the hair cell reveals a single tubulin-rich kinocilium (red, Fig. 5B,C) surrounded by a crescent of shorter actin-rich stereocilia (green, Fig. 5B,C); we define a polarity vector for each cell as an arrow pointing from the stereocilia to the kinocilium (Fig. 5C′).

To map hair cell polarities within the macula communis, we stained dissected stage 29 ears (25 dpf) with FITC-phalloidin and anti-acetylated tubulin antibody to mark the stereocilia and kinocilia, respectively (Fig. 5). The FITC-phalloidin stain revealed that lamprey hair cells have a substantial infracuticular network of actin penetrating into the hair cell body (Fig. 5B), which may correspond to the striated organelle described by Thornhill (Thornhill, 1972). This is not found in zebrafish hair cells, but a similar network has been described in guinea pig hair cells (Carlisle et al., 1988;

Slepecky, 1989); its function is unknown. We also observed shorter cilia projecting from all non-sensory cells of the otic epithelium, similar to those found in early zebrafish otic vesicles (Fig. 5C,D) (Riley et al., 1997).

To visualise polarity patterns within the macula, we mounted dissected *L. fluviatilis* ears such that each region of the epithelium was flattened for observation (Fig. 5E′,F′). It was not possible to flatten and visualise the entire macula communis in any one otic vesicle, so multiple ears were examined in overlapping units and the polarity maps combined, with overall 4× coverage. A summary of the pattern for *L. fluviatilis* is shown in Fig. 6. We also obtained a map of the anterior region of a single *P. marinus* embryo that is virtually identical to those obtained from *L. fluviatilis* (data not shown).

It is striking that the polarity map of the stage 29 *L. fluviatilis* macula shows a high degree of AP asymmetry: patterns in the anterior and posterior regions of the macula are quite distinct (Fig. 5E,F, Fig. 6). In the anterior region, hair cell polarities converge on a line that separates a smaller anterior domain from a larger posterior domain; in the posterior region, hair cell polarities diverge from a central line that bisects this region. In the extreme anterior and posterior domains of the posterior region, hair cells point anteriorly and posteriorly, respectively. Note that the map is flattened out; in the embryo, the anterior region of the macula actually folds up the anterior wall of the otocyst, so that the hair cells in this region actually point approximately ventrally and dorsally instead of posteriorly and anteriorly (see Fig. 5A for reference points). Beyond stage 29, however, the anterior region flattens down to lie on the ventral wall of the otocyst, so that eventually these hair cells will indeed point anteriorly and posteriorly (our observations of two stage 30 embryos) (Hagelin, 1974). Our data largely corroborate, but differ in detail to, the polarity patterns described in the larval *L. fluviatilis* ear using transmission electron microscopy (Thornhill, 1972).

In the adult *L. fluviatilis* macula, Lowenstein et al. (Lowenstein et al., 1968) report a similar pattern: most hair cells point anteriorly in the larger, anterior horizontal region, diverge from a midline in the vertical portion of the macula, and point posteriorly in the smaller, posterior horizontal region. Close examination of their data also reveals a small, posterior-facing domain in the anterior horizontal part of the macula. Thus hair cell polarity patterns in the stage 29 macula resemble those in the adult, but AP asymmetries in the pattern, particularly in the anterior portion of the macula, are much more evident at larval stages.

It is also noteworthy that the hair cell polarity patterns within the lamprey macula resemble those found in the embryonic zebrafish utricular and saccular maculae (Fig. 6) (Haddon et al., 1999). The anterior (utricular) macula of zebrafish consists mostly of roughly anterior-facing hair cells, with orientations fanning out from the medial side of the macula, abutting a thin stripe of posterior-facing hair cells, resembling the anterior region of the lamprey macula. The zebrafish posterior (saccular) macula consists mainly of a region of divergent polarities, with hair cells pointing dorsally and ventrally away from a central line, resembling the posterior region of the lamprey macula. There is one notable difference: the zebrafish embryonic saccular macula has an anterior extension with an antiparallel pattern of hair cell orientations, which does not correspond to any region of the lamprey pattern that we see. Overall,

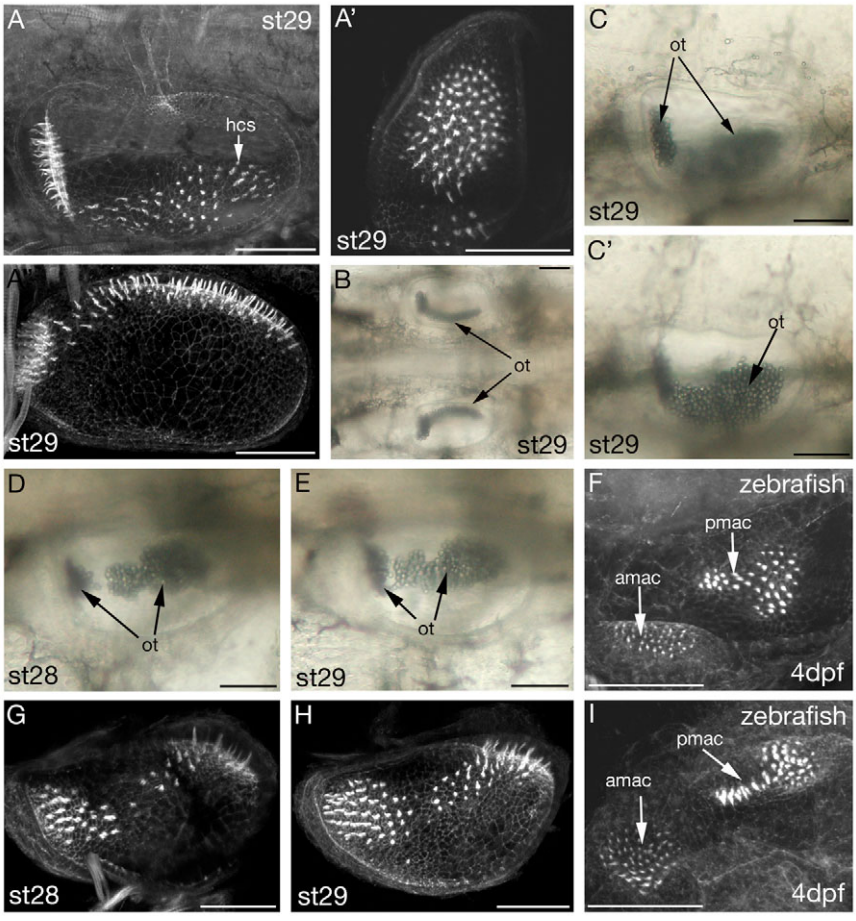

Fig. 3. Morphology of stage 28 and 29 *L. fluviatilis* ears, and comparison with zebrafish. (A-E,G,H) *L. fluviatilis*; (F,I) zebrafish, focussed medially to reveal maculae. amac, anterior macula; pmac, posterior macula (**A-A′′**,**F-I**) Projections of confocal *z*-stacks of FITC-phalloidin-stained ears revealing the actin-rich stereociliary bundles of the sensory hair cells (hcs). (**B-E**) DIC images of ears in the live lamprey larva. ot, otoconia. (A,C,C′,F) Lateral views, anterior to left, dorsal to top; (C,C′) different focal planes of the same specimen. (A′) Anterior view, dorsal to top, lateral to left. (A′′,B) Dorsal views, anterior to left; medial to top in A′′; both ears shown in B. (D,E,G-I) Dorsolateral views showing the join region between anterior and posterior areas of the macula; anterior approximately left. Scale bars: 50 μm.

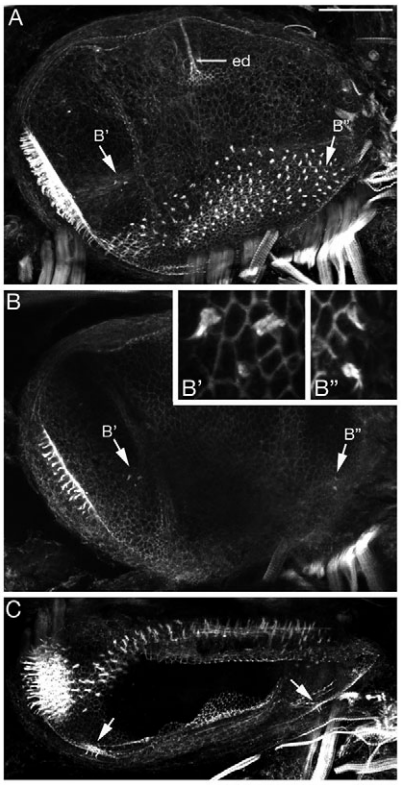

Fig. 4. Morphology of the *L. fluviatilis* otic vesicle at stage 30. (**A-C**) Projections from confocal *z*-stacks of a FITC-phalloidin-stained ear showing the actin-rich sensory hair cell stereociliary bundles and general morphology. (A,B) Lateral views, anterior to left, dorsal to top; both are composites of two images. ed, endolymphatic duct. (B) A projection from a lateral subset of the confocal *z*-stack to show the presumptive cristae clearly, also shown at higher power in insets (B′,B′′). (C) Dorsal view, anterior to left, medial to top; arrows indicate hair cells in the developing cristae. Scale bars: 50 μm.

however, our data suggest that the anterior and posterior regions of high hair cell density in the embryonic lamprey macula communis correspond closely to the utricular and saccular maculae, respectively, of the zebrafish. This interpretation is different to that suggested by Thornhill (Thornhill, 1972), that most of the anterior region of the embryonic macula contributes to the anterior crista.

Asymmetric expression of *tbx1* and *follistatin* is conserved in the lamprey otic vesicle

Having shown that the lamprey ear shows distinct morphological asymmetries about the AP axis from early stages, we wanted to see whether these are reflected in patterns of gene expression in the otic vesicle. We have used two genes that, although not directly implicated in the differentiation of maculae in the zebrafish, are clearly expressed in a polarised fashion in the otic epithelium in this species. In both the mouse and zebrafish otic vesicle, *Tbx1* is expressed in a posterolateral domain, with a clear border between posterior expressing cells and anterior non-expressing cells on the ventral side of the vesicle (Fig. 7A,C) (Piotrowski et al., 2003; Raft et al., 2004). *tbx1* expression has previously been reported in similar posterior regions of the *L. fluviatilis* otic vesicle (Sauka-Spengler et al., 2002). We have confirmed this in both *L. fluviatilis* and *P. marinus* (to which *L. fluviatilis tbx1* cross-hybridises) at stage 24-25. As in jawed vertebrate embryos, we see a clear boundary between anterior non-expressing and posterior *tbx1*-expressing cells in the lamprey otic vesicle, demonstrating that there is a very distinct asymmetry in the expression of this marker in the developing lamprey ear (Fig. 7B,D).

We also chose to examine *follistatin* expression in the lamprey ear, for two reasons. First, in zebrafish, *follistatin* expression marks a localised region of posterior otic cells from 24 hpf to at least 30 hpf (Fig. 7E) (Mowbray et al., 2001). Second, otic *follistatin* expression is lost in zebrafish embryos lacking Hh signalling, and is delocalised and duplicated at the anterior of the ear in embryos overexpressing Hh (Hammond et al., 2003). If the lamprey ear resembles these relatively symmetric ears generated by a disruption of Hh signalling in the zebrafish, we might expect to see a similar lack or duplication of *follistatin* expression in the lamprey otic vesicle. We amplified a single 301 bp *follistatin* fragment from *L. fluviatilis* stage 23-24 cDNA by degenerate PCR and then used this fragment to screen a 6- to 10-day *P. marinus* library (J. Langeland, Kalamazoo College). We obtained four positive plaques corresponding to two separate *follistatin* clones, one 1227 bp (one plaque) and one 1886 bp (three separate plaques). Both contain full-length open reading frames (ORFs) and a small region of 5′ UTR, with the larger also containing a large region of 3′ UTR. The predicted protein has 53.8% and 56.5% identity with zebrafish and mouse Follistatin proteins, respectively. These identities are based on the 1227 bp clone, as this contains an extra 81 bp that is not present in the larger cDNA but is present in the reported zebrafish and mouse genes (see Fig. S3 in the supplementary material).

Both *P. marinus* clones show identical expression patterns in stage 23 to 29 *P. marinus* embryos; the shorter clone also has the same expression pattern in *L. fluviatilis*. The longer clone, however, did not cross-hybridise, presumably because of the presence of the long 3′ UTR, which is likely to be less conserved than the ORF. There is 95.3% identity at the nucleotide level between the 301 bp *L. fluviatilis* fragment and the corresponding region of the shorter *P. marinus* clone, suggesting that the ORF has diverged relatively little between these two lamprey species.

Expression of *P. marinus follistatin* is seen in similar regions to zebrafish *follistatin*, in the branchial arches, somites and in the ear; a full expression pattern will be reported elsewhere. Expression in the vicinity of the otic vesicle begins at stage 23 when transcript is detected just posterior to the otic epithelium (Fig. 7G). At stage 24 and 25, strong *P. marinus follistatin* expression is seen throughout posterior regions of the otic epithelium, with a clear boundary between anterior non-expressing epithelium and the posterior *follistatin*-expressing area (Fig. 7F,H). No expression within the ear is seen at subsequent stages. The domain of *P. marinus follistatin* expression is similar to zebrafish *follistatin*: both genes mark posterior otic regions, confirming the molecular asymmetry of the lamprey otic vesicle. The expression of *P. marinus follistatin* is, however, more widespread in the posterior of the lamprey ear than the very discrete posterior *follistatin* domain seen in zebrafish (Fig. 7E). Nevertheless, we find no evidence of a duplicated pattern of expression, as in zebrafish embryos in which the Hh pathway has been over-activated.

Hh signal transduction is likely to be active in the lamprey otic vesicle

In the zebrafish, Hedgehog (Hh) signalling is crucial for posterior otic specification: as described above, embryos in which Hh signalling is disrupted can have mirror symmetric ears, consisting of two anterior or two posterior ends (Hammond et al., 2003). We initially hypothesized that the lamprey ear would be unresponsive to

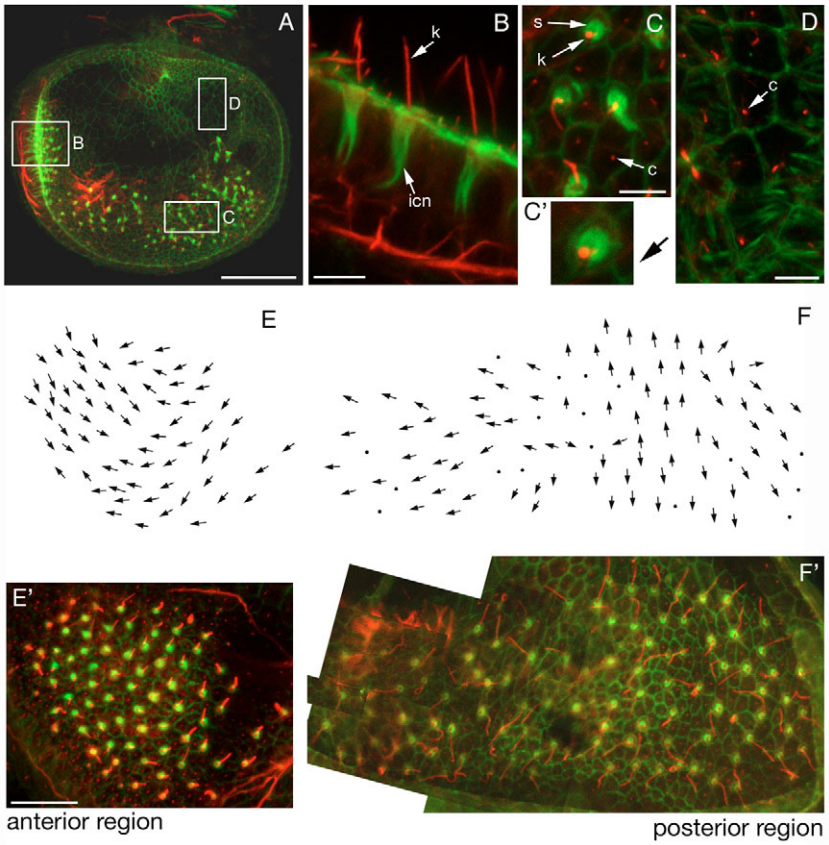

Fig. 5. Hair cell polarity in the macula communis of the *L. fluviatilis* ear at stage 29. (**A-D**) Projections from confocal *z*-stacks of FITC-phalloidin (green) and anti-acetylated tubulin (red) double stains revealing the actin-rich stereocilia and the tubulin-rich kinocilia of the sensory hair cells, respectively. (A) Lateral view of whole dissected-out inner ear; regions shown in boxes are the areas shown in detail in B, C and D. (B,C) Lateral (B) and dorsal (C) views of sensory epithelium showing the actin-rich infracuticular network (icn), the short apical horseshoe of stereocilia (s), the long kinocilia (k) and the short cilia (c) on non-sensory cells. (C′) Arrow, pointing from the stereociliary bundle towards the kinocilium, shows the polarity of one of the hair cells shown in C. (D) Non-sensory epithelium showing the short cilia (c) present on all non-sensory cells. (**E**,**F**) Polarity map of the anterior (E) and posterior (F) regions of the macula communis. (E′,F′) Stained and dissected specimen used to produce the map shown in E,F. F′ is a composite of several images taken in different focal planes. Scale bars: in A, 50 μm; in B-D, 5 μm; in E,F, 25 μm.

Hh signalling. However, as markers of otic AP asymmetry are shared between lamprey and zebrafish, we wanted to examine whether known otic AP patterning mechanisms might also be shared between the two species. To test whether the lamprey ear is responsive to Hh signalling we have examined *ptc* expression in the otic vesicle. *ptc* not only codes for the receptor for Hh signalling, but is also a transcriptional target of the Hh pathway; areas of strong *ptc* expression therefore indicate areas where active Hh signal transduction is occurring.

We isolated a 747 bp *ptc* fragment from the 6- to 10-day *P. marinus* cDNA library using degenerate PCR, and then screened the library with this fragment, isolating a single 1502 bp partial *ptc* clone. This has 48.4% and 48.3% identity with equivalent regions of zebrafish *ptc1* and *ptc2*, respectively, and 49.2% and 46.4% with mouse *ptc1* and *ptc2*. Phylogenetic analysis using CLUSTALW places the lamprey *ptc* clone equidistant in sequence from the *ptc1* and *ptc2* clusters of the gnathostome vertebrates, suggesting that there may be only a single *ptc* gene in lamprey (see Figs S4 and S5 in the supplementary material). *P. marinus ptc* is expressed in the brain, neural tube, somites and otic vesicle in a similar pattern to zebrafish *ptc1*; a full expression pattern will be reported elsewhere. In the lamprey otic vesicle, expression is seen from stage 23/24 to 25 in the ventromedial otic epithelium, suggesting that Hh signalling is indeed being transduced by these cells (Fig. 7J-L). This is similar to the expression of zebrafish *ptc1*, which is also seen in ventromedial otic epithelium up to 30 hpf (Fig. 7I) (Hammond et al., 2003). Although this evidence is circumstantial and does not prove that Hh signalling has a similar role in otic AP patterning of lamprey and zebrafish, it shows that a Hh signal is at least being transduced by similar regions of the otic vesicle in the two species.

Otx1 knockdown results in the fusion of the utricular and saccular maculae in the zebrafish inner ear

Having shown that otic vesicles in both lamprey and zebrafish are responsive to Hh signalling, we sought other candidate genes that may account for the differences in morphology between the lamprey and zebrafish ear. Acquisition of a role for Otx1 in the inner ear has previously been implicated in the evolution of the horizontal semicircular canal and crista in the gnathostome lineage (Mazan et al., 2000). Although the lamprey possesses an *otx* gene, it is not expressed in the developing ear, which lacks these structures (Ueki et al., 1998; Tomsa and Langeland, 1999). In the mouse, a loss of Otx1 function not only results in the loss of the horizontal semicircular canal, but also in the lack of constriction of the utriculo-saccular foramen, and incomplete segregation of the utricular and saccular maculae (Acampora et al., 1996; Morsli et al., 1999; Fritzsch et al., 2001). As our data suggest that regions of the lamprey macula communis correspond to the utricular and saccular maculae of zebrafish, we wanted to test whether a loss of Otx1 function in the zebrafish ear would result in the fusion of the utricular and saccular maculae, resulting in a lamprey-like macula communis.

We set out to test this hypothesis by knocking down Otx1 function in zebrafish embryos using an antisense morpholino (MO) designed to block splicing at the exon 3/4 boundary. We injected approximately 5 nl of either 0.66 mM or 1.0 mM *otx1* MO into one- to two-cell wild-type (WIK) zebrafish embryos. Similar otic phenotypes were obtained at both concentrations, although with a greater frequency in the higher concentration group [46% (n=74) and 97% (n=68) of ears, respectively]. All further experiments were performed at 1 mM. To measure the efficacy of the *otx1* MO, we carried out RT-PCR across the exon 3/4 splice junction at 24 hpf, 50

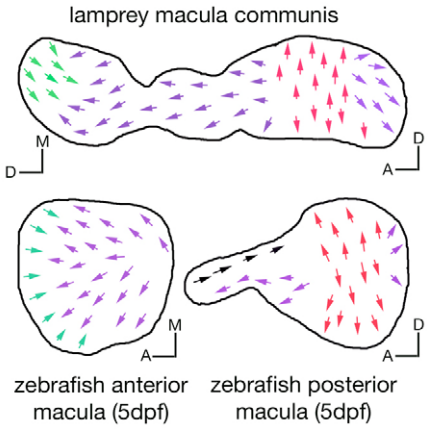

Fig. 6. Schematic representation and comparison of hair cell polarity maps of the lamprey macula communis, and of the anterior and posterior maculae of the developing zebrafish inner ear. The schematic representation of the hair cell polarity map of the lamprey macula communis is a summary of Fig. 5E,F. Maps of the anterior and posterior maculae of the developing zebrafish inner ear were produced using data from Haddon et al. (Haddon et al., 1999). Hair cells with similar orientations in the two species are shown in the same colour.

hpf, 74 hpf and 4 dpf, using cDNA produced from morphant and uninjected control embryos. We also used a primer pair directed to the actin gene as a positive control, which amplified a similar band from all samples (Fig. 8Q,R). The 447 bp *otx1* band amplified from wild-type samples represents the correctly spliced product. Initially, this is absent from *otx1* morphant samples, but begins to reappear by 48 hpf and is obvious at 74 hpf, suggesting that the efficacy of the morpholino is beginning to diminish by this time. The 471 bp and 408 bp bands amplified from the morphant samples represent aberrantly spliced products, where splicing has occurred from cryptic donor sites 39 bases 5′ or 24 bases 3′ of the correct exon 3 donor site. This was confirmed by sequencing the PCR products using internal primers (data not shown). Although neither of the aberrantly spliced products is predicted to cause a frame shift, the disrupted region is within the homeobox and is therefore likely to create a non-functional protein.

We examined the ears of live morphant embryos using DIC microscopy (Fig. 8A-D) and injection of a fluorescent tracer into the lumen of the vesicle to visualise the three dimensional morphology of the ear more clearly (Fig. 8E-H). For this, we used a control fluorescein-conjugated morpholino, as this is a large fluorescent molecule that will not leak out of the ear. We also used FITC-phalloidin staining to examine the ears of 3 and 4 dpf fixed embryos (Fig. 8K-P). In morphant ears, both the horizontal semicircular canal projection and crista are absent, and the anterior and posterior folds of tissue that separate the horizontal canal from the other canals are undivided (Fig. 8A-H). Fig. 8G,H clearly shows the lumens of only two canals (anterior and posterior) in morphant embryos compared with the wild-type three (anterior, posterior and horizontal). To confirm the loss of the horizontal crista, we examined the expression of *msxC*, which marks the developing cristae strongly. We detected only two expression domains – representing the anterior and posterior cristae – rather than the normal three in all of the 20 ears examined (Fig. 8I,J). Our data therefore indicate that the requirement for Otx1 function in the development of the horizontal canal and crista is conserved in the zebrafish.

The second striking aspect of the morphant phenotype concerns the positioning of the maculae. The anterior and posterior otoliths are, to varying extents, closer together than normal, reflecting the underlying fusion of the anterior (utricular) and posterior (saccular) maculae (Fig. 8K-P). The two maculae are still morphologically identifiable within the fused sensory area, suggesting that they have retained their AP identity despite the lack of non-sensory epithelium separating them. These data therefore support a role for Otx1 in the evolution of separate maculae in the gnathostome ear from an ancestral agnathan macula communis.

DISCUSSION

The developing lamprey otic vesicle has distinct asymmetries about the AP axis

At the onset of this study, we expected to find that the developing lamprey ear was relatively symmetric about the AP axis, based on previous descriptions of lamprey ear morphology. Two studies describe hair cell polarity patterns in the anterior and posterior horizontal regions of the late larval and adult *L. fluviatilis* macula communis as being almost symmetrical (Lowenstein et al., 1968; Thornhill, 1972). Hagelin proposes that both the horizontal regions of the macula communis are homologous to the utricular macula of gnathostomes (Hagelin, 1974), suggesting a double anterior ear. Our observations in the lamprey embryo, however, based on overall morphology, gene expression and hair cell polarity patterns, suggest that this is not the case: asymmetries in both the positioning of the embryonic macula and hair cell polarity patterns are exaggerated in the embryo compared with the adult. We have also shown that both *tbx1* and *follistatin* are expressed in a polarised fashion in both lamprey and zebrafish otic vesicles, suggesting that similar AP patterning mechanisms may function in the two species.

This pattern does not hold for all genes: *fgf8* is expressed at the anterior of the zebrafish otic vesicle, but the lamprey homologue, *fgf8/fgf17*, is not expressed in the otic vesicle of the Japanese lamprey, *Lampetra japonica* (Shigetani et al., 2002). We have cloned a similar fragment from *L. fluviatilis* and also see no otic expression (data not shown). This could be because *fgf8/fgf17* is not the true homologue of *fgf8*; however, this is unlikely, as phylogenetic analysis and other aspects of the *fgf8/fgf17* expression pattern suggest homology with zebrafish *fgf8* (Shigetani et al., 2002). Alternatively, it is possible that a different Fgf gene may perform the role of *fgf8* in the lamprey ear. It may be, however, that not all AP patterning mechanisms are shared between the lamprey and the zebrafish.

Regions of the developing macula communis appear to correspond to the utricular and saccular maculae of gnathostomes

Comparison of our stage 29 embryonic data with those of Lowenstein et al. (Lowenstein et al., 1968) (adult *L. fluviatilis*), Haddon et al. (Haddon et al., 1999) (5-day-old zebrafish) and Platt (Platt, 1993) (adult zebrafish), suggests that the anterior and posterior regions of the macula communis correspond to the utricular and saccular maculae of zebrafish, respectively. It is likely that this can be extrapolated to the utricular and saccular maculae of gnathostomes in general, as there are extensive similarities between polarity patterns in the various groups, although in most cases these have only been studied in the adult ear (Baird, 1974; Popper, 1978; Popper and Northcutt, 1983; Mathiesen and Popper, 1987; Platt, 1993; Denman-Johnson and Forge, 1999; Platt et al., 2004). The general pattern of polarity in the saccular macula, with hair cells pointing away from a central midline, is grossly similar to the adult

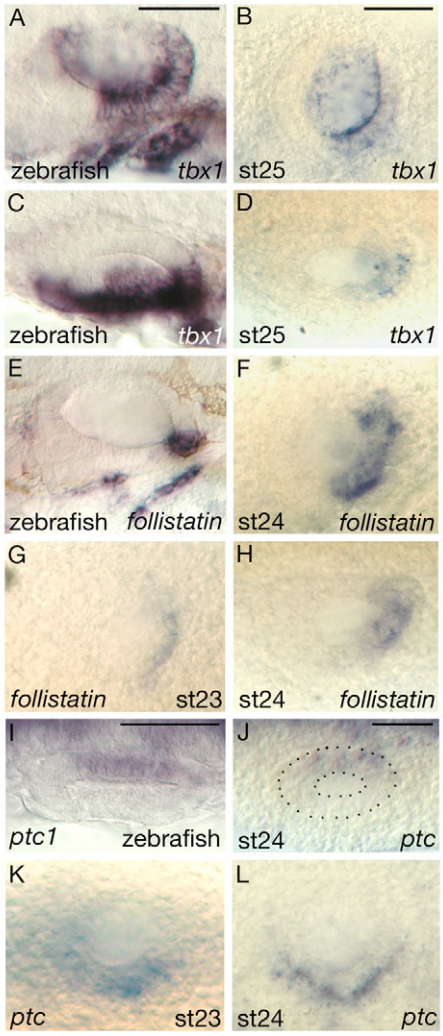

Fig. 7. Comparison of mRNA expression patterns.
(**A-L**) Comparison of the mRNA expression patterns of *tbx1*, *follistatin* and *ptc* in zebrafish and lamprey (*P. marinus*) otic vesicles. (A,C) 28 hpf zebrafish; (E) 30 hpf zebrafish; (I) 20 hpf zebrafish; all others are *P. marinus* at the stages shown. (C,D,H-J) Dorsal views, anterior to left, medial to top; all others are lateral views, anterior to left, dorsal to top. The otic vesicle is outlined in J for clarity. Scale bars: in A, 50 μm for A,C,E; in B, 50 μm for B,D,F-H,K,L; in I,J, 50 μm.

zebrafish pattern in all adult gnathostomes examined, although the shape of this organ varies dramatically between groups. In most gnathostome species, the adult utricular macula also has a very similar polarity pattern to the adult zebrafish pattern. The utricular macula of the Chondrichthyes differs, however, consisting of intermingled hair cells of opposing polarity (Baird, 1974).

In zebrafish, the third otolithic endorgan, the lagenar macula, is thought to arise de novo at around day 15, rather than being prefigured by either the anterior (utricular) or posterior (saccular) macula (Platt, 1993; Bang et al., 2001; Bever and Fekete, 2002). Two different areas of the adult lamprey macula have previously been proposed to correspond to the lagenar macula. These are the central vertical region (de Burlet and Versteegh, 1930; Hagelin, 1974) and the posterior horizontal region (Lowenstein et al., 1968). Our work suggests that there is no direct equivalent of the lagenar macula in the lamprey by stage 29; it is also unlikely to arise later, as all areas of the adult macula polarity pattern seem to be present in the stage 29 macula (Fig. 5) (Lowenstein et al., 1968). In the absence of saccular and lagenar macula-specific markers, however, it is difficult to be certain about these homologies.

The lagena is much more variable between gnathostome groups than either the saccule or the utricle. Polarity patterns differ, with some groups (e.g. sturgeon, bichir and gar) having a variation on the theme of an antiparallel array, and others (e.g. teleosts and bowfins) displaying a pattern similar to that of the utricle (Popper, 1978; Popper and Northcutt, 1983; Mathiesen and Popper, 1987; Platt, 1993). In other instances, notably the holocephalans and elasmobranchs, the lagena is absent or rudimentary, with varying degrees of separation from the saccular macula (Baird, 1974). In many tetrapods, including mammals, the lagena seems to have been lost altogether. Thus the evolution of this endorgan is not straightforward, perhaps having evolved or been secondarily lost more than once, as has previously been suggested (Fritzsch, 1992).

Acquisition of a role for *otx1* in the developing gnathostome inner ear can account for all major differences between agnathan and gnathostome inner ears

We now know that our Hh loss- and gain-of-function otic phenotypes in the zebrafish (Hammond et al., 2003) do not appear to resemble the lamprey ear. We also find that a transcriptional target of the Hh pathway, *ptc*, is expressed in the ventromedial otic vesicle of both lamprey and zebrafish, suggesting that an AP patterning mechanism based on Hh signalling may be present in the lamprey. Similarly, although a loss of *Tbx1* function in the mouse gives rise to a more symmetric ear (Raft et al., 2004), conserved expression of *tbx1* at the posterior of the lamprey otic vesicle suggests that an otic AP patterning mechanism based on Tbx1 function may be shared by both species.

The major difference between lamprey and gnathostome ears, therefore, is not one of symmetry about the AP axis, but concerns the structural arrangement of the semicircular canals and maculae. In addition to the lack of a horizontal semicircular canal and crista, the sensory macula is undivided in lampreys but split into two separate patches in zebrafish. It has been noted that the utriculo-saccular duct is less constricted in mice lacking Otx1 function, and that the saccular and utricular maculae are incompletely segregated (Morsli et al., 1999; Fritzsch et al., 2001). In the zebrafish Otx1 morphants, the utricular and saccular maculae are also juxtaposed, forming a single macula communis. Notably, however, AP polarity is not lost in these ears: the phenotype is quite different to the 'twinned' macula seen in our Hh loss- and gain-of-function experiments (Hammond et al., 2003). Thus it appears that the loss of Otx1 function in the zebrafish, rather than a disruption of Hh signalling, results in an ear that resembles that of the lamprey. Therefore, the acquisition of *otx1* expression in the otic vesicle – a new domain of expression of an existing transcriptional regulator – can account for both of the major differences in inner ear morphology between lampreys and gnathostomes.

When did AP polarity in the ear arise?

Our analysis of the developing lamprey ear suggests that an otic vesicle with distinct AP polarity, similar to that in the zebrafish, was already present in the common ancestor of these species. Can we extrapolate this to the more general assertion that the common ancestor of the gnathostomes and the agnathans had an ear with a distinct otic AP polarity?

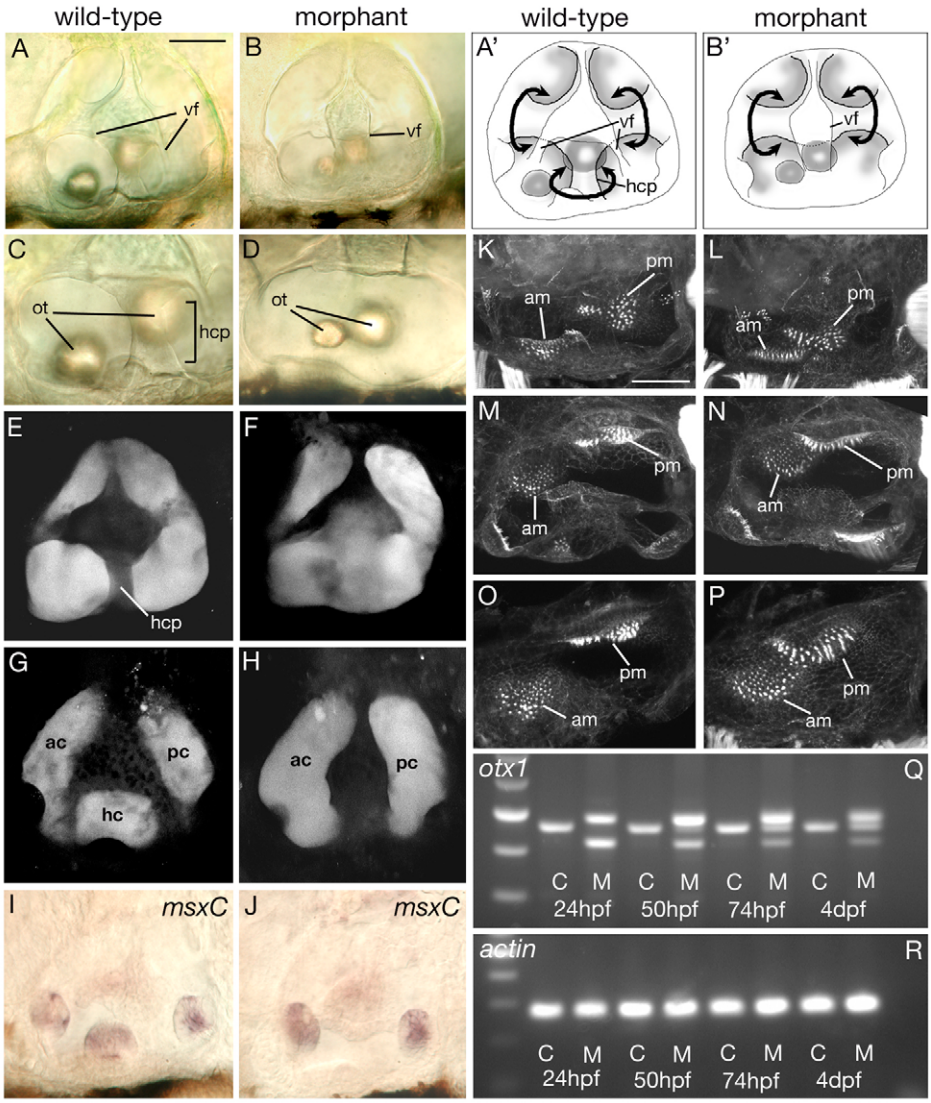

Fig. 8. Effects on the developing ear of injection of *otx1* morpholino into wild-type zebrafish embryos. (**A-D**) DIC images of ears of live embryos. (A′,B′) Schematic representation of ears shown in A,B. Note the lack of the horizontal canal projection (hcp) that delimits the horizontal semicircular canal and the fusion of the two ventral folds (vf) in morphant embryos. The otoliths (ot) of morphants are also closer together than in wild type. Curved black arrows indicate the semicircular canal lumens. (**E-H**) Confocal sections through ears in which the lumens have been filled with fluorescein-conjugated morpholino. (E,F) Medial sections, in the plane of the semicircular canal projections; (G,H) Lateral sections, in the plane of the lumens of the semicircular canals. ac, anterior canal; pc, posterior canal; hc horizontal canal. (**I,J**) mRNA expression pattern of *msxC* marking the cristae. (**K-P**) Projections of confocal *z*-stacks of FITC-phalloidin-stained ears revealing the actin-rich stereocilia of the sensory hair bundles. am, anterior macula; pm, posterior macula. (A-L) Lateral views, dorsal to top; (M,N) dorsal views, medial to top; (O,P) junction between anterior and posterior maculae. Anterior is to the left in all panels. All ears are at 96 hpf, except I and J, which are 72 hpf. Scale bars: 50 μm. (**Q**) RT-PCR across the exon 3/4 boundary. Lane 1, 100 bp ladder; brightest band is 500 bp. (**R**) RT-PCR using primers to actin. C, control uninjected siblings; M, morpholino-injected embryos.

The gnathostomes form a monophyletic group, but it is less clear whether the extant agnathans also form a monophyletic group, or whether lampreys are a sister group to the gnathostomes, with the hagfish forming a more basal outgroup. Molecular data tend to support the monophyly of lampreys and hagfish, whereas morphological data, particularly when extinct lineages are taken into account, suggest that the jawless vertebrates are very unlikely to be a monophyletic group (Janvier, 1996) (reviewed by Meyer and Zardoya, 2003). We can therefore conclude that the common ancestor of the gnathostomes and lamprey, but not necessarily of all vertebrates, was likely to have had an otic vesicle with distinct otic AP polarity similar to that seen in the zebrafish.

We cannot exclude the possibility that the common ancestor of extant gnathostomes and agnathans had a mirror symmetric ear, and that the enantiomorphic ears produced by genetic or physical disruptions of gnathostome embryos are indeed atavistic phenotypes. It is also possible that hagfish embryos have a more symmetrical otic vesicle than do lamprey embryos, and that this represents the ancestral form. Nevertheless, hagfish appear to have many uniquely derived characteristics, and, as such, may not be representative of a common ancestor (Janvier, 1996; Mallatt and Sullivan, 1998). As hagfish are deep-sea fish, their embryos are extremely difficult to obtain, and we have not been able to examine ear development in this species.

No evidence of otic placodes has yet been found in the cephalochordates, a non-vertebrate chordate group (Kozmik et al., 1999; Streit, 2001). However, in ascidians, the basal non-vertebrate chordate group, Mazet et al. (Mazet et al., 2005) present persuasive molecular evidence that the atrial siphon of *Ciona* and its associated cupular organs are homologous to the inner ear of vertebrates. The homology of these structures was initially proposed based on morphological criteria and was later corroborated by observation of expression of a *pax2/pax5/pax8* homologue in larvae in regions destined to form the atria (Jefferies, 1969; Bone and Ryan, 1978; Wada et al., 1998). Mazet et al. (Mazet et al., 2005) now show that a panel of markers homologous to genes expressed in the vertebrate inner ear, including *foxIc*, as well as members of the Pax, Eya and Six families, mark two ectodermal regions on either side of the posterior brain of embryonic and larval *Ciona*. These regions go through a thickened phase resembling placodes before invaginating to form the atrial openings. It will be of interest to see whether these structures, which appear to represent the first evolutionary step towards a vertebrate inner ear, show any signs of AP polarity.

We would like to thank David McCauley (Caltech), Susan and Brian Morland (Belflask Ecological Survey Team), and Seb Shimeld (Oxford) enormously for much enthusiastic help and advice with lamprey embryo collection, which went well above and beyond the call of duty. We would also like to thank Sylvie Mazan (Paris), Shigeru Kuratani (RIKEN) and Jim Langeland (Kalamazoo) for generously sharing probes and reagents, and Matthew Holley and Philip Ingham for critical reading of the manuscript. We also thank the Forestry Commission of Great Britain, the Environment Agency and English Nature for access to lamprey spawning sites, and Fiona Browne and Lisa Gleadall for care of the zebrafish facility. This work was supported by the BBSRC (50/G19428).

Supplementary material

Supplementary material for this article is available at
http://dev.biologists.org/cgi/content/full/133/7/1347/DC1

References

Acampora, D., Mazan, S., Avantaggiato, V., Barone, P., Tuorto, F., Lallemand, Y., Brûlet, P. and Simeone, A. (1996). Epilepsy and brain abnormalities in mice lacking the *Otx1* gene. *Nat. Genet.* **14**, 218-222.

Avallone, B., Fascio, U., Senatore, A., Balsoamo, G., Bianco, P. G. and Marmo, F. (2005). The membranous labyrinth during larval development in lamprey (*Lampetra planeri*, Bloch, 1784). *Hear. Res.* **201**, 37-43.

Baird, I. L. (1974). Some aspects of the comparative anatomy and evolution of the inner ear in submammalian vertebrates. *Brain Behav. Evol.* **10**, 11-36.

Bang, P., Sewell, W. and Malicki, J. (2001). Morphology and cell type heterogeneities of the inner ear epithelia in adult and juvenile zebrafish (*Danio rerio*). *J. Comp. Neurol.* **438**, 173-190.

Bever, M. M. and Fekete, D. M. (2002). Atlas of the developing inner ear in zebrafish. *Dev. Dyn.* **223**, 536-543.

Bone, Q. and Ryan, K. P. (1978). Cupular sense organs in *Ciona* (Tunicata: Ascidiacea). *J. Zool. Lond.* **186**, 417-429.

Carlisle, L., Zajic, G., Altschuler, R. A., Schacht, J. and Thorne, P. R. (1988). Species differences in the distribution of infracuticular F-actin in outer hair cells of the cochlea. *Hear. Res.* **33**, 201-206.

de Burlet, H. M. and Versteegh, C. (1930). Über bau und funktion des Petromyzonlabyrinthes. *Acta Otolaryngol. Suppl.* **13**, 1-58.

Denman-Johnson, K. and Forge, A. (1999). Establishment of hair bundle polarity and orientation in the developing vestibular system of the mouse. *J. Neurocytol.* **28**, 821-835.

Fritzsch, B. (1992). The water-to-land transition: evolution of the tetrapod basilar papilla, middle ear, and auditory nuclei. In *The evolutionary biology of hearing* (ed. D. B. Webster, A. N. Popper and R. R. Fay), pp. 351-375. New York: Springer-Verlag.

Fritzsch, B., Signore, M. and Simeone, A. (2001). *Otx1* null mutant mice show partial segregation of sensory epithelia comparable to lamprey ears. *Dev. Genes Evol.* **211**, 388-396.

Gegenbaur, C. (1898). Vergleichende Anatomie der Wirbelthiere mit Berücksichtigung der Wirbellosen. Leipzig: Wilhelm Engelmann.

Haddon, C. and Lewis, J. (1996). Early ear development in the embryo of the zebrafish, *Danio rerio*. *J. Comp. Neurol.* **365**, 113-123.

Haddon, C., Mowbray, C., Whitfield, T., Jones, D., Gschmeissner, S. and Lewis, J. (1999). Hair cells without supporting cells: further studies in the ear of the zebrafish *mind bomb* mutant. *J. Neurocytol.* **28**, 837-850.

Hagelin, L. O. (1974). Development of the membranous labyrinth in lampreys. *Acta Zool. Suppl.* 1-218.

Hammond, K. L., Loynes, H. E., Folarin, A. A., Smith, J. and Whitfield, T. T. (2003). Hedgehog signalling is required for correct anteroposterior patterning of the zebrafish otic vesicle. *Development* **130**, 1403-1417.

Harrison, R. G. (1936). Relations of symmetry in the developing ear of *Amblystoma punctatum*. *Proc. Natl. Acad. Sci. USA* **22**, 238-247.

Harrison, R. G. (1945). Relations of symmetry in the developing embryo. *Trans. Conn. Acad. Arts Sci. USA* **22**, 238-247.

Janvier, P. (1996). *Early vertebrates.* New York: Oxford University Press.

Jefferies, R. P. S. (1969). *Ceratocystis perneri* Jaekel – a middle Cambrian chordate with echinoderm affinities. *Palaeontology* **12**, 494-535.

Kozmik, Z., Holland, N. D., Kalousova, A., Paces, J., Schubert, M. and Holland, L. Z. (1999). Characterization of an amphioxus paired box gene, *AmphiPax2/5/8*: developmental expression patterns in optic support cells, nephridium, thyroid-like structures and pharyngeal gill slits, but not in the midbrain-hindbrain boundary region. *Development* **126**, 1295-1304.

Léger, S. and Brand, M. (2002). Fgf8 and Fgf3 are required for zebrafish ear placode induction, maintenance and inner ear patterning. *Mech. Dev.* **119**, 91-108.

Lowenstein, O. (1971). The labyrinth. In *Fish Physiology* (ed. W. S. Hoar and D. J. Randall), pp. 207-240. London; New York: Academic Press.

Lowenstein, O. and Thornhill, R. A. (1970). The labyrinth of *Myxine*: anatomy, ultrastructure and electrophysiology. *Proc. R. Soc. Lond. B* **176**, 21-42.

Lowenstein, O., Osborne, M. P. and Thornhill, R. A. (1968). The anatomy and ultrastructure of the labyrinth of the lamprey (*Lampetra fluviatilis* L.). *Proc. R. Soc. Lond. B* **170**, 113-134.

Mallatt, J. and Sullivan, J. (1998). 28S and 18S rDNA sequences support the monophyly of lampreys and hagfishes. *Mol. Biol. Evol.* **15**, 1706-1718.

Mathiesen, C. and Popper, A. N. (1987). The ultrastructure and innervation of the ear of the Gar, *Lepisosteus osseus*. *J. Morph.* **194**, 129-142.

Mazan, S., Jaillard, D., Baratte, B. and Janvier, P. (2000). *Otx1* gene-controlled morphogenesis of the horizontal semicircular canal and the origin of the gnathostome characteristics. *Evol. Dev.* **2**, 186-193.

Mazet, F., Hutt, J. A., Milloz, J., Millard, J., Graham, A. and Shimeld, S. M. (2005). Molecular evidence from *Ciona intestinalis* for the evolutionary origin of vertebrate sensory placodes. *Dev. Biol.* **282**, 494-508.

McCauley, D. W. and Bronner-Fraser, M. (2002). Conservation of Pax gene expression in ectodermal placodes of the lamprey. *Gene* **287**, 129-139.

Meyer, A. and Zardoya, R. (2003). Recent advances in the (molecular) phylogeny of vertebrates. *Annu. Rev. Ecol. Evol. Syst.* **34**, 311-338.

Morsli, H., Tuorto, F., Choo, D., Postiglione, M. P., Simeone, A. and Wu, D. K. (1999). *Otx1* and *Otx2* activities are required for the normal development of the mouse inner ear. *Development* **126**, 2335-2343.

Mowbray, C., Hammerschmidt, M. and Whitfield, T. T. (2001). Expression of BMP signalling pathway members in the developing zebrafish inner ear and lateral line. *Mech. Dev.* **108**, 179-184.

Nehls, M., Pfeifer, D. and Boehm, T. (1994). Exon amplification from complete libraries of genomic DNA using a novel phage vector with automatic plasmid excision facility: application to the mouse neurofibromatosis-1 locus. *Oncogene* **9**, 2169-2175.

Piotrowski, T., Ahn, D.-G., Schilling, T. F., Nair, S., Ruvinsky, I., Geisler, R., Rauch, G.-J., Haffter, P., Zon, L. I., Zhou, Y. et al. (2003). The zebrafish *van gogh* mutation disrupts *tbx1*, which is involved in the DiGeorge deletion syndrome in humans. *Development* **130**, 5043-5052.

Platt, C. (1993). Zebrafish inner ear sensory surfaces are similar to those in goldfish. *Hear. Res.* **65**, 133-140.

Platt, C., Jorgenson, J. M. and Popper, A. N. (2004). The inner ear of the lungfish *Protopterus*. *J. Comp. Neurol.* **471**, 277-288.

Popper, A. N. (1978). Scanning electron microscopic study of the otolithic organs in the Bichir (*Polypterus bichir*) and Shovel-nose Sturgeon (*Scaphirhynchus platorynchus*). *J. Comp. Neurol.* **181**, 117-128.

Popper, A. N. and Northcutt, R. G. (1983). Structure and innervation of the inner ear of the Bowfin, *Amia calva*. *J. Comp. Neurol.* **213**, 279-286.

Raft, S., Nowotschin, S., Liao, J. and Morrow, B. (2004). Suppression of neural fate and control of inner ear morphogenesis by *Tbx1*. *Development* **131**, 1801-1812.

Riley, B. B., Zhu, C., Janetopoulos, C. and Aufderheide, K. J. (1997). A critical period of ear development controlled by distinct populations of ciliated cells in the zebrafish. *Dev. Biol.* **191**, 191-201.

Sauka-Spengler, T., Le Mentec, C., Lepage, M. and Mazan, S. (2002). Embryonic expression of *Tbx1*, a DiGeorge syndrome candidate gene, in the lamprey *Lampetra fluviatilis*. *Gene Exp. Patt.* **2**, 99-103.

Shigetani, Y., Sugahara, F., Kawakami, Y., Murakami, Y., Hirano, S. and Kuratani, S. (2002). Heterotopic shift of epithelial-mesenchymal interactions in vertebrate jaw evolution. *Science* **296**, 1316-1319.

Slepecky, N. (1989). An infracuticular network is not required for outer hair cell shortening. *Hear. Res.* **38**, 135-140.

Streit, A. (2001). Origin of the vertebrate inner ear: evolution and induction of the otic placode. *J. Anat.* **199**, 99-103.

Tahara, Y. (1988). Normal stages of development in the lamprey, *Lampetra reissneri* (Dybowski). *Zool. Sci.* **5**, 109-118.

Thornhill, R. A. (1972). The development of the labyrinth of the lamprey (*Lampetra fluviatilis* Linn. 1758). *Proc. R. Soc. Lond. B* **181**, 175-198.

Tomsa, J. M. and Langeland, J. A. (1999). *Otx* expression during lamprey embryogenesis provides insights into the evolution of the vertebrate head and jaw. *Dev. Biol.* **207**, 26-37.

Ueki, T., Kuratani, S., Hirano, S. and Aizawa, S. (1998). Otx cognates in a lamprey, *Lampetra japonica*. *Dev. Genes Evol.* **208**, 223-228.

Wada, H., Saiga, H., Satoh, N. and Holland, P. W. (1998). Tripartite organization of the ancestral chordate brain and the antiquity of placodes: insights from ascidian *Pax-2/5/8*, *Hox* and *Otx* genes. *Development* **125**, 1113-1122.

Waldman, E., Lim, D. and Collazo, A. (2001). Ablation studies on the developing inner ear reveal a propensity for mirror duplications. *Assoc. Res. Otolaryngol. Abs.* **24**, 76.

Westerfield, M. (1995). *The Zebrafish Book: a guide for the laboratory use of zebrafish (*Danio rerio*)*. Oregon: University of Oregon Press.